

ACTIVE VIBRATION CONTROL OF SMART PLATES BY USING PIEZOELECTRIC
ACTUATORS

Yavuz Yaman

Department of Aerospace Engineering, Middle
East Technical University, 06531, Ankara, Turkey
yyaman@metu.edu.tr

Volkan Nalbantoğlu
ASELSAN Electronics
Industries, Akyurt, 06011, Ankara
Turkey
vналbant@mgeo.aselsan.com.tr

David Waechter

Sensor Technology Limited P. O. Box 97 Steward
Road, Collingwood, Ontario, Canada L9Y3Z4
dwaechter@sensortech.ca

Tarkan Çalışkan

Department of Aerospace Engineering, Middle
East Technical University, 06531, Ankara, Turkey
tarkan@ae.metu.edu.tr

Demet Ülker
Department of Aerospace
Engineering, Middle East
Technical University, 06531,
Ankara, Turkey
dulker@ae.metu.edu.tr

Eswar Prasad
Sensor Technology Limited
P. O. Box 97 Steward Road,
Collingwood, Ontario, Canada
L9Y3Z4

eprasad@sensortech.ca
BinYan

Sensor Technology Limited P. O. Box 97 Steward
Road, Collingwood, Ontario, Canada L9Y3Z4
binyan@sensortech.ca

ABSTRACT

A finite element based modeling technique is presented for a smart fin (flat plate with surface bonded piezoelectric actuators). By using ANSYS®(v.5.6) software, this study first gives the effects of the piezoelectric patches on the response of the smart fin, then also explains the influence of actuator size, placement and determines the optimum sensor locations. The smart fin is then used in the determination of an identified model from experimental data. Based on this model an H_∞ controller is designed to suppress in-vacuo vibrations due to the first two modes of the smart fin. The effectiveness of the technique in the modeling of uncertainties is also shown. It has been shown that the controller guaranties the robust performance of the system in the presence of uncertainties.

NOMENCLATURE

$\ \cdot \ _\infty$	Infinity norm of a signal or system
$\bar{\sigma}(M)$	Maximum singular value of matrix M
P	Nominal plant model
K	Controller
Δ	Norm bounded uncertainty block
F_l	Lower linear fractional transformation form
μ	Structured singular values for a system

Other parameters are clearly defined wherever applicable.

1. INTRODUCTION

Recent developments in the field of piezoelectric materials have encouraged many researchers to work in the field of smart structures. A smart structure can be defined as the one which can sense the external disturbance and respond to that with active control in real time to maintain the mission requirements. These structures consist of highly distributed active devices and processor networks. The active devices are primarily sensors and actuators either embedded or attached to an existing passive structure.

The research on the application of the smart structures in active vibration control was initiated by Bailey (Bailey and Hubbard, 1985). Utilization of discrete piezoelectric actuators has been shown to be a viable concept for vibration suppression. Crawley (Crawley and de Luis, 1989) proposed an analytical solution for a static case including various actuator geometries. They stated that discrete piezoelectric actuators could be considered in vibration suppression of some modes of vibration of flexible structures. Kalaycıoğlu (Kalaycıoğlu and Misra, 1992) developed a dynamic modeling technique for vibration suppression of plate structures by using PZT patches. The technique developed incorporates geometrical and mechanical properties of the actuator with the structures on which they are mounted.

The application of the finite element modeling techniques in the smart materials technologies is in continuous growth during the last decade. Hence it gains a certain evolution so that some piezoelectric elements have become available in commercial finite element codes like ANSYS®.

The finite element method was shown to be a very effective tool for the analysis of the smart structures by Wang (Wang and Jen, 1996). Unlike the analytical techniques, the method offers fully coupled thermo-mechanical-electrical analysis of the smart structures. This allows the prediction of the reciprocal relations between the sensors and actuators. This allowance makes the development of the closed loop controller for active vibration control possible, (Prasad *et al.*, 1996). Using the time-delay techniques developed by Kalaycıoğlu (Kalaycıoğlu *et al.*, 1997), the effectiveness of the smart materials on the active control of space structures are shown. In one of the recent studies Suleman (Suleman and Costa, 1998) proposed the effectiveness of the piezoceramic sensor and actuators on the suppression of vibrations on an experimental wing due to gust loading.

Yaman (Yaman *et al.*, 2001) worked on the finite element based modeling technique for the determination of the system model of the smart beam. Based on this model, they designed an H_∞ controller which effectively suppresses the vibrations of the smart beam due to its first two modes. In their work, the suitability of the H_∞ design technique in the modeling of uncertainties and the evaluation of the robust performance of the system were also demonstrated.

At the initial stages of the design the finite element model is sufficient. The finite element modeling allows the

determination of the optimal actuator and sensor placement, actuator size and power requirements. Generally, finite element method accurately predicts the natural frequencies and mode shapes of the structure. Since the technique makes no damping predictions, it determines transfer functions relating the inputs and the outputs of the systems not very accurately.

Because of the difficulties in the development of an accurate finite element model of the smart structure, the technique is considered at the design stage instead; hence an experimentally identified model is used for the controller design.

This study presents the active vibration control technique applied to a smart fin, which is composed of an aluminum flat plate modeled in cantilever configuration and with active PZT patches. Using experimentally identified model, an H_∞ controller that effectively suppresses vibrations of the smart fin due to its first two modes is designed. The effectiveness of the technique in the modeling of the uncertainties is also presented.

2. FINITE ELEMENT MODELING OF THE SMART FIN

In the theoretical analysis, finite element code ANSYS® (v5.6) was used. During the development of the smart fin, a model having parametric design capability is created.

The only suitable element having piezoelectric capacity in three dimensional coupled field problems is the solid type element (SOLID5). Similar to other structural solid elements the element has three displacement degrees of freedoms per node. In addition to these degrees of freedoms, the element has also potential degrees of freedoms. Piezoceramic actuators inherently exhibit anisotropy and yield three dimensional spatial variation in their response to piezoelectric actuation. Therefore, the models developed for the passive portion should include consistent degrees of freedoms with the actuator degrees of freedom at the locations where these elements interface.

Theoretically, the plate elements (shell or solid) can be used in the modeling of the passive portion of the smart structure. While the shell elements can be used in accordance with the thin plate theory, the solid elements work with the three dimensional elasticity theories.

Therefore, the utilization of solid type elements in the modeling of the passive portion allows the calculation of the effects of the normal stresses and the transverse shear stresses which may be developed in the passive portion of the smart structures.

Although solid and shell elements possess different degrees of freedoms, these elements can be used in the same model. This can be achieved through the application of appropriate coupling strategies between the nodes of concern. This guarantees the transfer of the nodal forces corresponding to nodal displacements at the locations where solid and shell elements interfaces. In this case however, the nodal forces corresponding to nodal rotations do not transfer (ANSYS, 2000).

Yaman (Yaman *et. al.*, 2001) investigated the influences of the element type selection on the response of the smart structures. In this work, it is shown that the use of shell elements in the modeling of the passive portion leads to the inaccurate calculation of the global stiffness matrix. The modeling of the passive portion using consistent solid elements with the actuator elements however, is determined to yield accurate results.

In this work, solid elements (SOLID5) are used for the modeling of the active portion (piezoelectric actuators) and compatible solid elements (SOLID45) are used for the passive portion (aluminum plate).

Effects of Actuator placement

The influence of placement of $24 \times (25 \times 25 \times 0.5)$ mm BM500 type actuators on the aluminum fin is considered. The anisotropic material, piezoelectric and dielectric properties of BM500 type actuators are prescribed by the manufacturer, Sensor Technology Ltd (Sensor Technology Ltd., 2001). By using the modal analysis results, the actuators are placed on the aluminum fin. In this work, the identically polarized patches are assumed to be bonded symmetrically on both top and bottom surface of the fin. The finite element model developed in the study is shown in Figure 1.

Figure 2 gives the theoretical static response of the smart fin to various piezoelectric actuation values. The first two theoretically determined natural frequencies and mode shapes are shown in Figure 3

In order to determine the influences of the actuator placement on the response, two cases are considered. At each one, by keeping the distances between the piezoelectric patches fixed, the x and y positions of all actuators are varied from their original configuration given in Figure 1 in x and y directions respectively. The results in terms of the right tip corner displacements are given in Figure 4.

It is evident from the figure that as the patches are moved away from the root ($y=0$) along y direction on the fin the response reduces for both bending and twisting actuation. This is due to the higher strain developed near the root. For this reason, the patches should be placed on the fin as close as possible to the root. Furthermore, as the patches are moved away from the leading edge ($x=0$) the bending response remains less effected and the twisting response reduces due to the reduction of the twisting arm which is the maximum x distance between the actuators. In order to improve the twisting response this distance should be maximized.

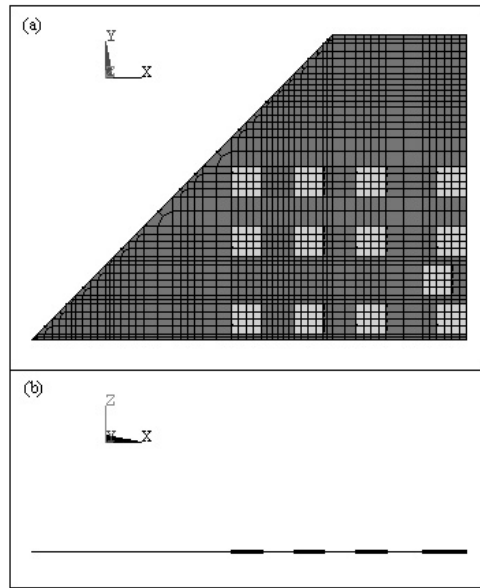


Figure 1. The finite element model developed in the study
1.a. Top view
1.b. Side view

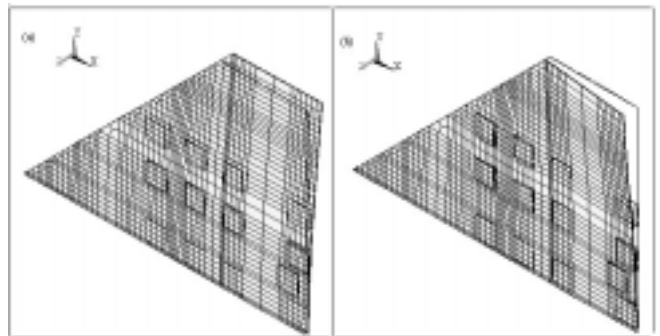


Figure 2. The theoretical response of the smart fin to various piezoelectric actuation values
2.a. Bending by 300V
2.b. Twisting by +300V and -300V

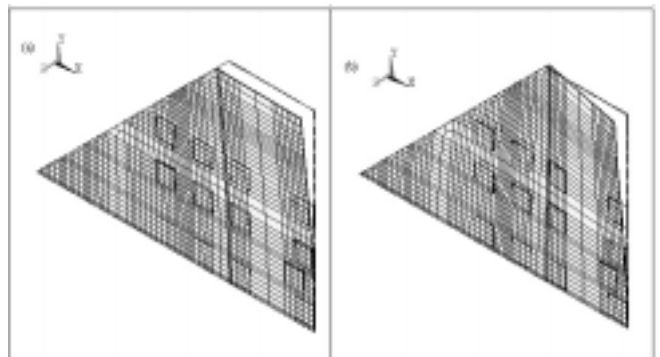


Figure 3. The first two theoretical mode shapes of the smart fin
3.a. The first mode ($f_1=14.963$ Hz)
3.b. The second mode ($f_2=45.737$ Hz)

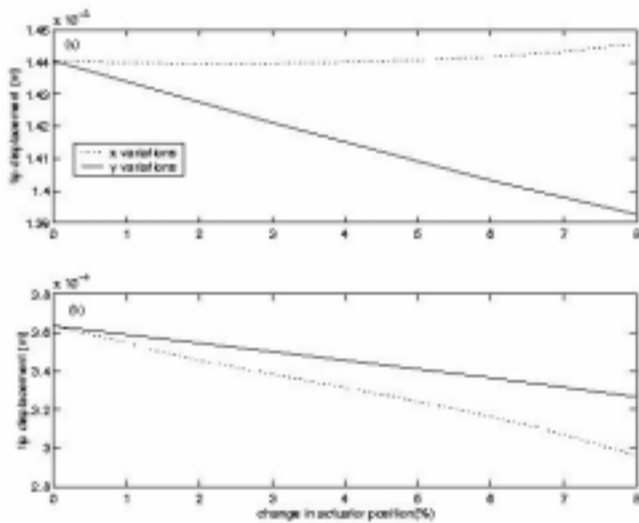


Figure 4. The influences of the actuator placement on the response . (the increase in the x or y locations)

4.a. Bending (by 300V)

4.b. Twisting (by +300V and -300V)

The influences of the actuator placement on the first two natural frequencies of the smart fin are also investigated and the results are shown in Figure 5.a and Figure 5.b. It can be seen from these figures that, while the x variations of the actuator positions do not appreciably affect the first natural frequency, it increases the second natural frequency. The y variations in the actuator positions however, reduce both first and the second natural frequencies.

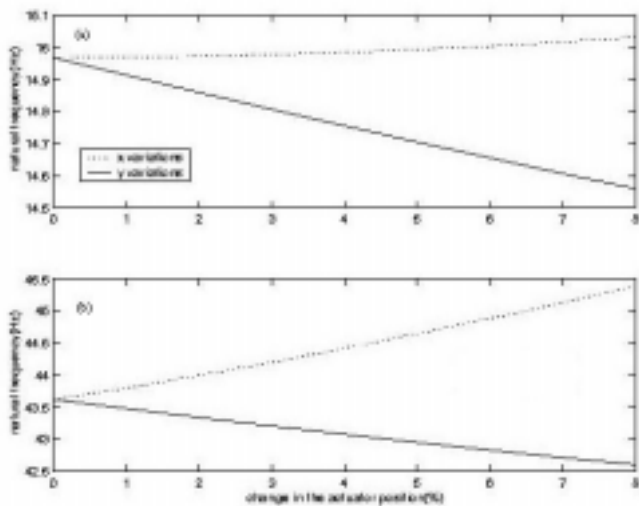


Figure 5. The influences of the actuator placement on the first two theoretical natural frequencies of the smart beam(increase in the x and y locations)

5.a. First natural frequency

5.b. Second natural frequency

The influences of the Actuator Size on the Response

Depending on the mission requirements, the size of the piezoelectric actuators can be altered. The effects of the increase in the size of the actuator on the response in terms of the change in the coverage ratio are investigated. The coverage ratio is defined as the ratio of the area of the fin covered by the piezoelectric actuators. Using the original configuration of the smart plate, the coverage ratio is increased and the results for the piezoelectric actuation of 300V are shown in Figure 6. Although the increase in the length of the actuators makes smart fin stiffer, it also increases the energy transmitted to the smart fin giving a rise to the response for the specified piezoelectric actuation value.

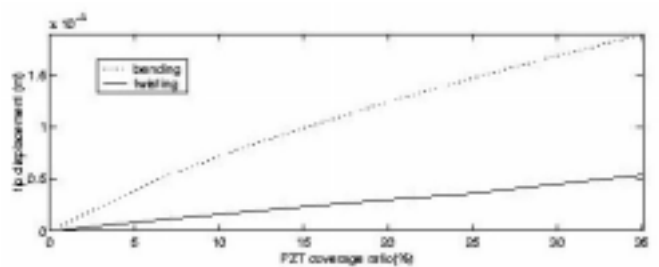


Figure 6. The comparison of the effects of the actuator size variation on the response of the smart fin (right tip corner response at 300V)

The Maximum Admissible Piezoelectric Actuation

Because piezoelectric materials have tensile strengths in the order of 63 MPa, they are brittle. Therefore, the stress in the actuators can be critical in adverse applications. In order to determine the maximum piezoelectric actuation value, Von Mises stresses developed in the actuators for various actuation values should be investigated prior to operation. For this reason, Von Mises stresses for various actuation type and voltages are calculated and results are shown in Figure 7. Since, Von Mises stresses are in the order of 10 MPa for normal operating conditions (200-300V), the piezoelectric actuators are not expected to fail.

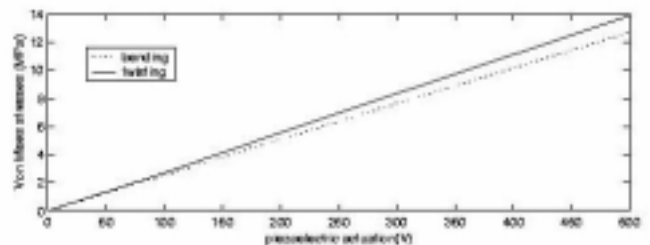


Figure 7. The effect of the piezoelectric actuation voltage variation on the Von Mises stresses developed within the piezoelectric actuators.

The Influence of the Transverse and Normal Stresses

The modeling of the passive portion by using compatible solid elements not only guaranties the proper transfer of the nodal forces generated by the active elements on the passive elements at the interface where these elements meet, but also allows the computation of the transverse shear and normal stresses developed on the passive portion of the smart fin due to the piezoelectric actuation.

In order to investigate the importance of these stresses, using the original configuration of the smart fin, the maximum stresses developed on the passive portion of the smart fin by the piezoelectric actuation in bending or twisting are calculated. Figures 8 and 9 give the variation of the stress components as a function of the piezoelectric actuation voltage. For the twisting actuation, shear stress in yz plane is the maximum shearing stress component in twisting. Therefore, the exclusion of these stresses, hence using shell elements, may lead to inaccurate results

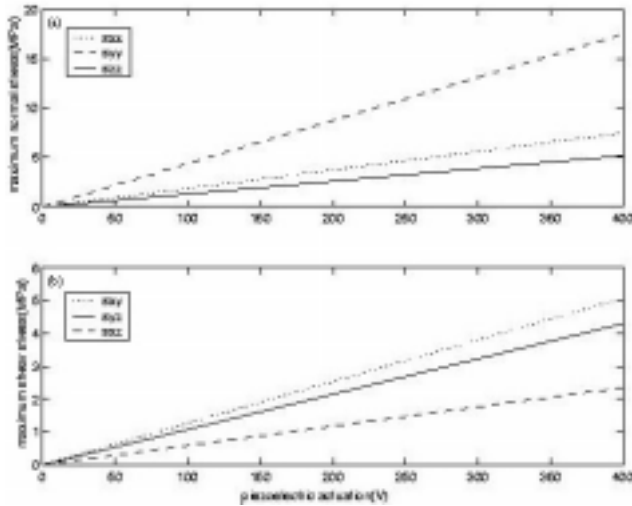


Figure 8. The comparison of the effects of the voltage variation on the maximum stresses developed on the passive portion of the smart fin due to the piezoelectric actuation in bending (s_{xx} , s_{yy} , s_{zz} are the maximum normal stress component along x, y and z directions respectively s_{xy} , s_{yz} , s_{xz} are the maximum shearing stress component on xy, yz and xz planes respectively)

- 8.a. The normal stresses
- 8.b. The shearing stresses

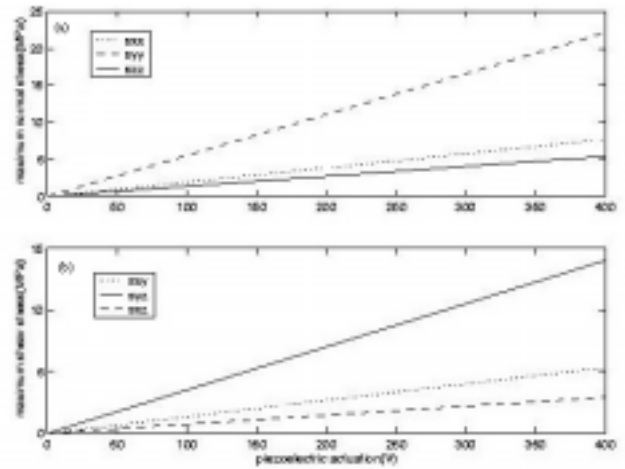


Figure 9. The comparison of the effects of the voltage variation on the maximum stresses developed on the passive portion of the smart fin due to the piezoelectric actuation in twisting (Legend Figure 8)

- 9.a. The normal stresses
- 9.b. The shearing stresses

Placement of Strain Gages

Finite element method allows the determination of the most suitable locations of the sensors for active vibration control. These locations can be determined by the utilization of mode shapes of the smart structure. In this work, by using the modal analysis results of the smart fin, three locations are determined for the strain gage sensors to sense vibrations of the smart fin due to its first two modes. The optimum locations so obtained and the configuration of the strain gages and the piezoelectric sensors on the smart fin are shown in Figure 10. In this model, while the strain gage at location (1) is used for the measurement of strain in x direction, locations (2) and (3) are considered in the measurement of the strain in y direction.

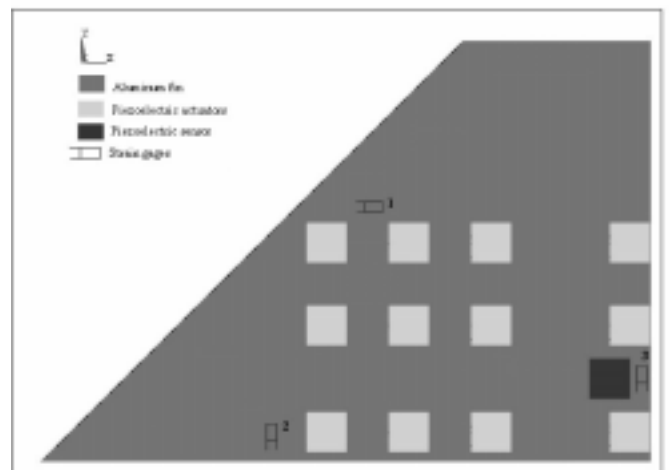


Figure 10. The placement and the configuration of the strain gages and piezoelectric patches on the smart fin

In order to investigate the effectiveness of the piezoelectric actuators and the strain gage sensors, the static response of the smart fin to the piezoelectric actuation is considered. Using the initial size and configurations of the actuator patches, the influences of the piezoelectric actuation voltage variation on the responses at the three sensor locations are calculated for both bending and twisting piezoelectric actuation. Figure 11 gives the results in terms of the magnitude of the strain at the measurement locations. It can be seen from these figures that for bending and twisting actuation the highest response is calculated at location (2).

Since the theoretical model is in the linear range of the piezoelectricity and the effects of the large deflections are considered to be negligible, the response of the smart fin is found to vary linearly with the actuation voltage.

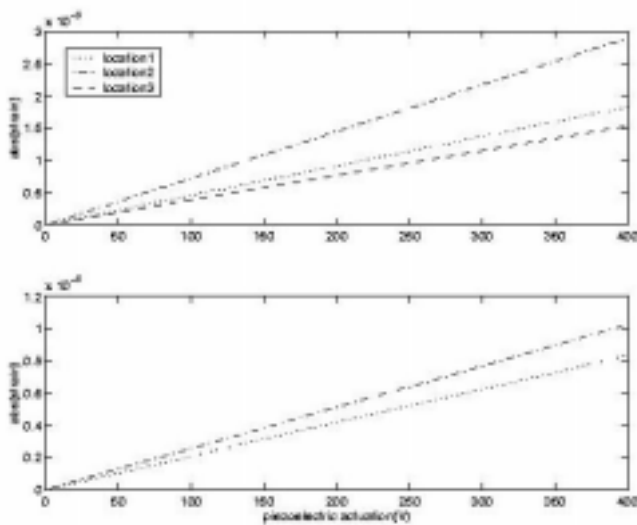


Figure 11. The comparison of the variation of the piezoelectric actuation on the response of the smart fin (location (1): ϵ_x locations (2) and (3): ϵ_y)
 11.a. Bending by 300V
 11.b. Twisting +300V and -300V

The Test Article

By using the results obtained from the theoretical analysis for the smart fin, the test article was produced.

The test article was produced and tested at Sensor Technology Limited of Canada. The smart fin model consists of 24x(25x25x5 mm) symmetrically placed BM500 type piezoelectric actuators. It further contains 6 symmetrically placed SG-7 LY13 type strain gages (Omega Engineering CT) to sense the bending and torsional vibrations. An additional symmetrically placed BM500 type piezoelectric sensors are also used. The test article is shown in Figure 12.

In the current study, as a result of the analysis explained in Section 2, only strain gage sensors labeled (1) and (2) are used in the extraction of the experimental transfer functions. Furthermore, during the experiments bending actuation is applied to one face of the smart fin.

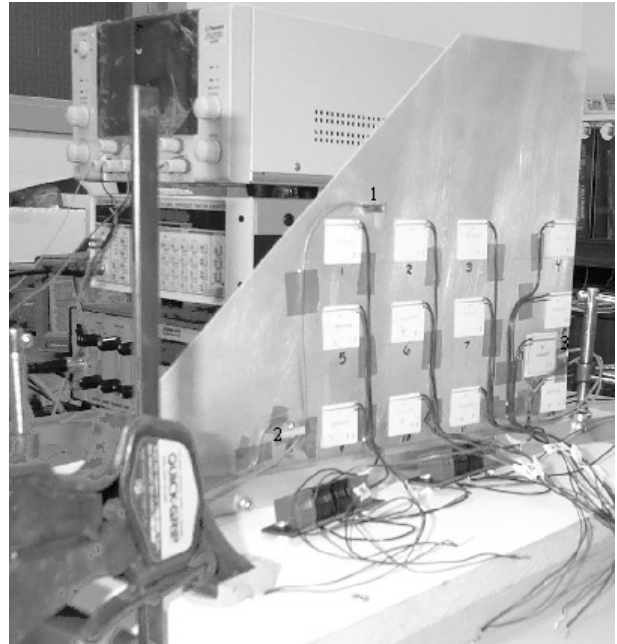


Figure 12. The test article used in the study

Table 1 gives the comparison of the undamped theoretical (FEM) and the experimental resonance frequencies together with the modal damping ratios (ζ_r) at the first three modes of the smart fin.

The discrepancies in the resonance frequencies can be attributed to the unmodelled cable weights and the actual damping present in the smart fin

Frequencies (Hz)	FEM	Experimental	ζ_r
f_1	14.963	14.51	4.8004e-2
f_2	45.737	48.94	2.023e-1
f_3	68.253	69.43	1.7923e-2

Table 1. The comparison of the theoretical and experimental resonance frequencies of the smart fin

3. SYSTEM IDENTIFICATION

An accurate model of the input/output behavior of the system is required for controller design. One way to achieve this is the utilization of the finite element modeling technique. However, due to the difficulties in the determination of an accurate finite element model for the smart fin, technique is considered to be less effective compared to the system identification technique, (Dosch, Leo and Inmann, 1995). In the system identification technique, the most convenient system model to be used in the controller design is obtained by using the curve fitting a transfer function model to each single-input/single-output (SISO) experimental frequency response functions. These transfer functions are then combined to form a

multivariable representation of the structure, (Nalbantoğlu, 1998). The application of this technique results in 6th order transfer functions from the actuators to each sensor. The comparisons of these models with the experimental transfer functions are shown in Figures 13-14

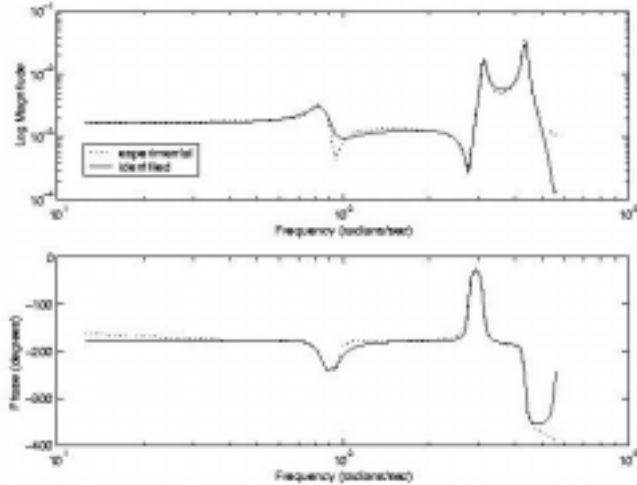


Figure 13. The comparison of the experimental and identified models for the strain gage sensor pairs at location 1

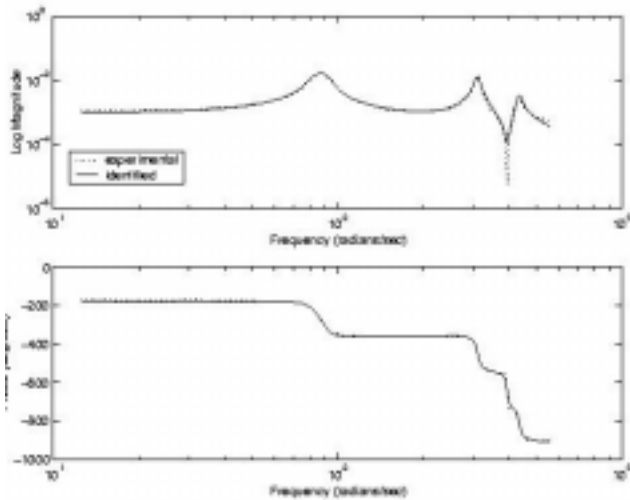


Figure 14. The comparison of the experimental and identified models for the strain gage sensor pairs at location 2

4. H_∞ CONTROLLER DESIGN

Based on the model obtained in Section 3, an H_∞ controller is designed for the smart fin. The goal of the controller is to attenuate the vibrations of the fin at its first two natural frequencies (in the range from zero to 60 Hz) and gain stabilize the unmodeled high frequency modes.

In H_∞ control design framework, the objective is to minimize the H_∞ norm of the weighted transfer functions from the input disturbance signals to the output error signals, (Doyle *et. al.*, 1992) and (Zhou *et. al.*, 1996). The uncertainties in the

plant model can be put in such a form that some of the disturbances and error signals correspond to the channels through which the nominal model interacts with a norm bounded uncertainty block Δ . This generates the set of plants in which the true plant is assumed to exist. This framework is represented in Figure 15.

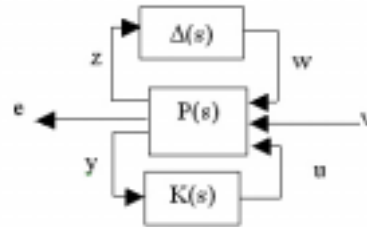


Figure 15. The modeling of uncertainties

Here, P is the nominal plant model with appropriate weights to reflect the design goals, K is the controller to be designed, and Δ is the norm bounded uncertainty block, v is a vector of exogenous inputs such as reference commands, disturbances and noise, e is a vector of error signals to be kept small, y is a vector of sensor measurements and u is a vector of control signals, w and z are the disturbance and error channels corresponding to the uncertainty block Δ respectively.

For the design purposes, the Δ block is eliminated and the input-output map from $[w \ v]^T$ to $[z \ e]^T$ is expressed in lower linear fractional transformation form $F_1(P, K)$ as

$$\begin{bmatrix} z \\ e \end{bmatrix} = F_1(P, K) \begin{bmatrix} w \\ v \end{bmatrix} \quad (1)$$

Where, $F_1(P, K) = P_{11} + P_{12} K(I - P_{22} K)^{-1} P_{21}$

Assuming that plant P is partitioned according to the dimensions of the control, measurement, disturbance and error signals, as

$$P = \begin{bmatrix} P_{11} & P_{12} \\ P_{21} & P_{22} \end{bmatrix} \quad (2)$$

The objective is to find a stabilizing controller K that minimizes the ∞ -norm of $\|F_1(P, K)\|_{\infty}$. For an uncertainty block satisfying $\|\Delta\|_{\infty} < 1$ the closed loop system in Figure 14 has robust performance if $\|F_1(P, K)\|_{\infty} \leq 1$ is achieved, (Zhou and Doyle, 1996).

This result, however, is conservative because it assumes that the delta block is a full block with no structure to it. The uncertainties in a realistic problem are due to the components of a system, and representation of such uncertainties results in a block diagonal Δ . A less conservative robustness test for the closed loop system is given by examining the structured singular values (μ) of $M = F_1(P, K)$. For a given system M and an uncertainty structure, structured singular value μ is defined by Doyle and Zhou (Doyle and Zhou, 1996), and μ -

Analysis and Synthesis toolbox of the commercial program Matlab®(v.6.0, 2001).

$$\mu_{\Delta} = \frac{1}{\min\{\overline{\sigma}(\Delta) : \Delta \in \Delta', \det(I - M\Delta) = 0\}} \quad (3)$$

where Δ' is the set of block diagonal matrices

If no $\Delta \in \Delta$ makes $(I - M\Delta)$ singular then $\mu_{\Delta}(M) = 0$

For an appropriately weighted control design formulation, a μ value of less than one across all frequencies indicates robust performance.

The H_{∞} controller synthesis and μ -analysis techniques described above are applied to the smart fin.

In H_{∞} controller design for the smart fin, the performance objective is to minimize the maximum frequency response of the first two modes of the smart fin at the sensor locations. Figure 16 shows the formulation of the closed loop control in H_{∞} framework.

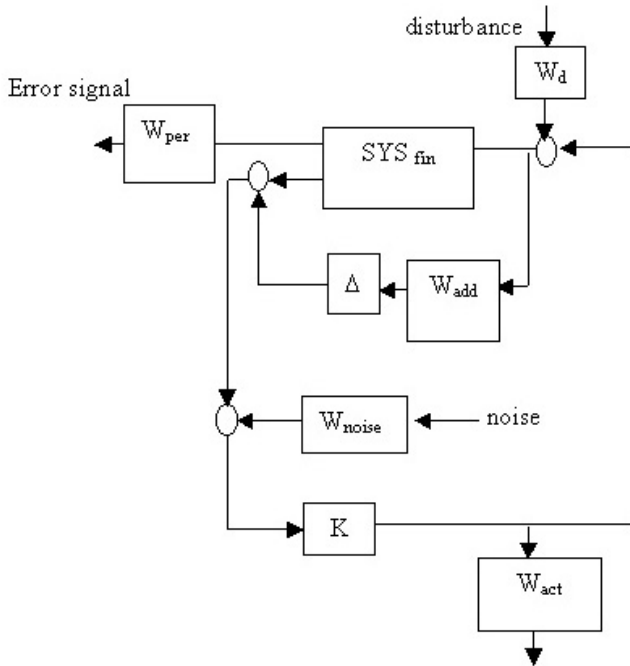


Figure 16. The block diagram formulation of the control problem

In Figure 16, SYS_{fin} defines the nominal smart fin model, W_{per} represents a performance weight on the strain gage sensors to achieve the performance objective. For both strain gage output channels, magnitude of the W_{per} weights are shown in Figure 17. These weights are selected to achieve attenuation in the peak frequency response of the closed loop system.

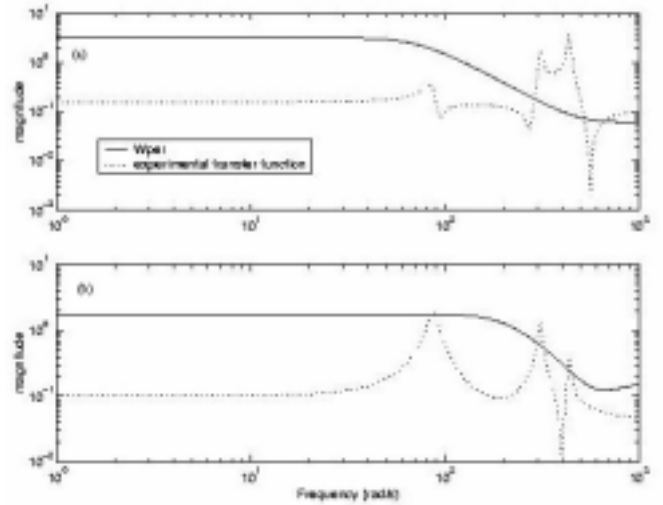


Figure 17. The comparison of the performance weight W_{per} and the experimental transfer function at the strain gage locations
17.a. Location (1)
17.b. Location (2)

An additive uncertainty is included in the problem formulation to account for the unmodeled high frequency modes and modeling errors inside the controller bandwidth. This weight is selected to have a magnitude greater than the structural modes above 500 rad/sec. If robust stability of the closed-loop system is achieved for this additive uncertainty model, the flexible modes of the structure will be gain stabilized above 500 rad/sec. Figure 18 shows the magnitude of W_{add} versus the singular value plot of the transfer function from the piezoelectric actuators to both strain gage sensors.

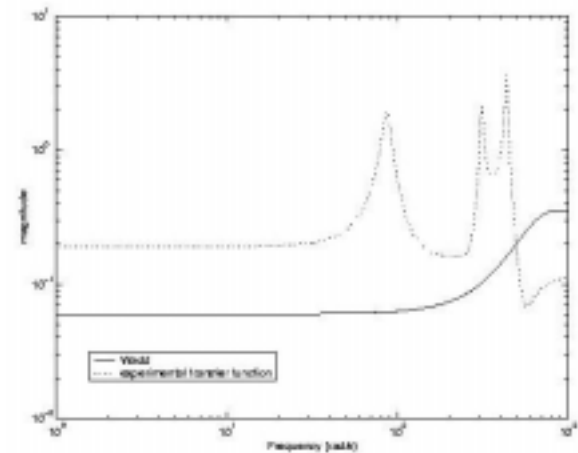


Figure 18. The comparison of the additive weight W_{add} and the experimental transfer function at the location (1).

To limit the actuator command signal in the control design process to 250 volts W_{act} in Figure 16 is chosen as 1/250. The weights on the disturbance input, W_{dist} is taken to be 1. This indicates that the input disturbance is expected to be on the

same order of magnitude as the controller signals. The strain gage signals have a signal to noise ratio of 100 on both channels, therefore, W_{noise} in Figure 16 is taken as a 2×2 diagonal matrix with 0.01 as the diagonal elements. A 12th order controller is obtained by applying the standard solution techniques to the system formulated in Figure 16. This controller is tested on a 10th order model of the smart fin obtained from the experimental data by using system identification as explained in Section 3. Open and closed loop frequency responses for both channels are shown in Figure 19 and Figure 20. The μ - analysis results are given in Figure 21

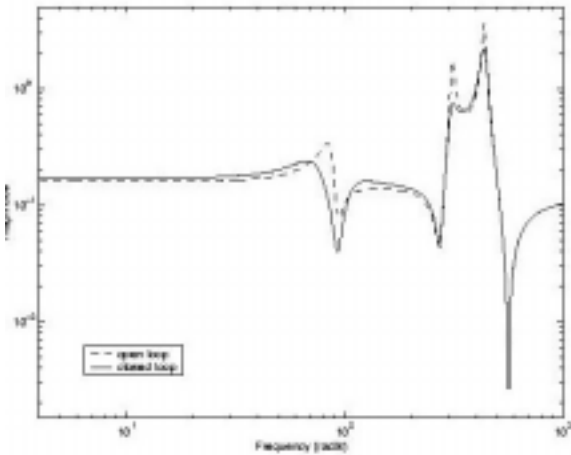


Figure 19. The comparison of the open and closed loop responses of the smart fin for the strain gages at location (1)

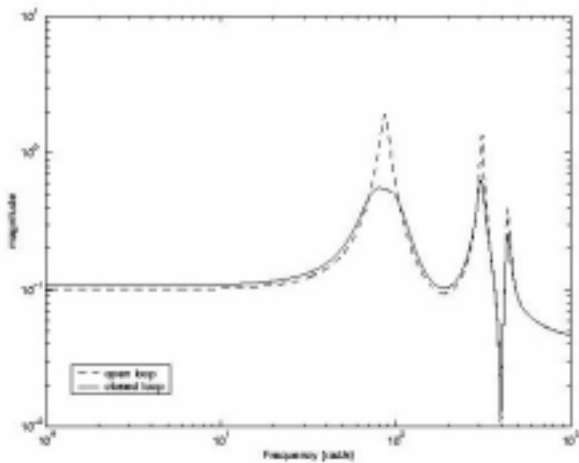


Figure 20. The comparison of the open and closed loop responses of the smart fin strain gages for the strain gages at location (2)

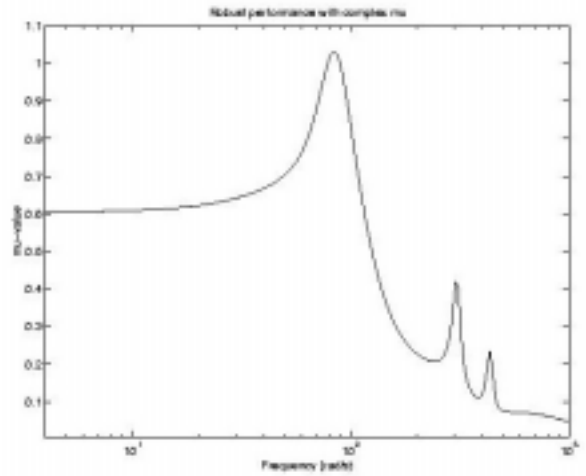


Figure 21. Structural singular value (μ) of the closed loop system.

In Figure 21, a peak value of μ approximately equal to one indicates that the desired robust performance objectives are achieved. Frequency response of the controller is given in Figure 22.

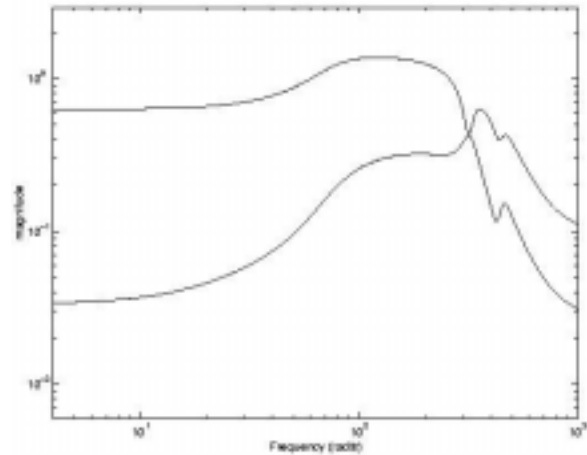


Figure 22. The frequency responses of the controller

μ has a peak value of approximately one. This indicates that the robust performance requirements are satisfied for the closed loop system.

The attenuation levels (open loop/closed loop peak values) of the first, second and third modes for the first and second channels are 1.5, 2.3, 1.5 and 3.5, 2.1, 1.5 respectively.

5. CONCLUSIONS

A study was presented for active vibration control of a smart fin. Based on the finite element modeling technique, the study addressed issues in the determination of the influence of the placement and size of the piezoceramic actuators. This leads to the determination of the most suitable locations for the piezoelectric actuators and the strain gages.

Because of the difficulties in the development of an accurate finite element model of the smart fin, an experimentally identified model of the smart fin was utilized in the design of H_{∞} controller which suppresses in-vacuo vibrations of the smart fin due to its first two modes. The effectiveness of the technique in the modeling of uncertainties was also shown. It was shown that the controller guarantees the robust performance of the system in the presence of uncertainties.

6. ACKNOWLEDGMENTS

This work was supported by NATO/RTO/Applied Vehicle Technology Panel through the project T-121 'Application of Smart Materials in the Vibration Control of Aeronautical Structures'. The authors gratefully acknowledge the support given.

7. REFERENCES

Bailey, T. Hubbard, J. E. 1985, "Distributed Piezoelectric-Polymer Active Vibration Control of a Cantilever Beam." *Journal of Guidance, Control and Dynamics*, Vol.8, No. 5, pp 605-611.

E. F. Crawley, J. Louis, "Use of Piezoelectric Actuators as Elements of Intelligent Structures." *AIAA Journal*, October 1989.

S. Kalaycıoğlu and A. Misra "Approximate Solutions for Vibrations of Deploying Appendages." *Journal of Guidance Control and Dynamics*, *AIAA_14* (2), 1991

S. Kalaycıoğlu, M. M. Giray and H. Asmer, "Time Delay Control of Space Structures Using Embedded Piezoelectric Actuators and Fiber optic Sensors." *SPIE's 4th Annual Symposium on Smart Structures and Materials*, March 1997

A. Suleman, A. P. Costa, C. Crawford, R. Sedaghati, "Wind Tunnel Aeroelastic Response of Piezoelectric and Aileron Controlled 3-D Wing." *CanSmart Workshop Smart Materials and Structures Proceedings*, Sep. 1998

Wang and C. K. Jen, "Design and Fabrication of Composites for Static Shape Control." *Final_Report, NRC-CNRC*, 1996

S. E. Prasad, J.B. Wallace, B. E. Petit, H. Wang C. K. Jen. Kalaycıoğlu, M. Giray "Development of Composite Structures for Static Shape Control." *SPIE, Far East and Pacific Rim Symposium on Smart Materials, Structures and MEMS*. (Bangor, India)

ANSYS[®] User's Manual (version 5.6), *ANSYS Inc. Southpointe 275 Technology Drive Canonsburg, PA 15317*.

Y. Yaman, T. Çalışkan, V. Nalbantoğlu, D. Waechter, E. Prasad, "Active Vibration Control of a Smart Beam." *Canada-US CanSmart Workshop Smart Materials and Structures proceedings*, oct. 2001 Montreal Quebec Canada
Sensor Technology Ltd. *Product Data Sheets*, 2001

V. Nalbantoğlu, *Ph.D. Thesis*, University of Minnesota, 1998, "Robust Control and System Identification for flexible structures"

J. Dosch, J. Inmann, "Modeling and Control for Vibration Suppression of a Flexible Active Structure." *Journal of Guidance, Control and Dynamics*, Vol. 8, April 1995"

J. Doyle, B. Francis and A. Tanenbaum, "Feedback Control Theory." Mac Millan publishing, New York, 1992

K. Zhou, J.C. Doyle, K. Glover "Robust and Optimal Control." Prentice Hall, New Jersey, 1996

G. Balas, J. Doyle, K. Glover, A. Packard, *Matlab[®](v.6.0) μ -Toolbox Users's Manual*